Ye, X. & Slabaugh, G.G. (2011). Concavity analysis for reduction of ileocecal valve false positives in CTC. Paper presented at the 8th IEEE International Symposium on Biomedical Imaging: From Nano to Macro, 30-03-2011 - 02-04-2011, Chicago, USA.

CITY UNIVERSITY LONDON
EST 1894

City Research Online

Original citation: Ye, X. & Slabaugh, G.G. (2011). Concavity analysis for reduction of ileocecal valve false positives in CTC. Paper presented at the 8th IEEE International Symposium on Biomedical Imaging: From Nano to Macro, 30-03-2011 - 02-04-2011, Chicago, USA.

Permanent City Research Online URL: http://openaccess.city.ac.uk/4376/

CONCAVITY ANALYSIS FOR REDUCTION OF ILEOCECAL VALVE FALSE POSITIVES IN CTC

Xujiong Ye and Greg Slabaugh

Research and Development Department, Medicsight PLC, London, W14 8UD, UK

ABSTRACT

The ileocecal valve (ICV) is a common source of false-positive (FP) detections in CT colonography (CTC) computer-aided detection (CAD) of polyps. In this paper, we propose an automatic method to identify ICV CAD regions to reduce FPs. The ICV is a particularly challenging structure to detect due to its variable, polyp-mimicking morphology. However, the vast majority of ICVs have a visible orifice, which appears as a 3D concave region. Our method identifies the orifice concave region using a partial differential equation (PDE) based on 3D curvature and geometric constraints. These orifice features, combined with intensity and shape features generated in a Bayesian framework, comprise a set of compact features fed into an Adaboost classifier to produce a final classification of a region being ICV or non-ICV. Experimental results on a multi-center tagged CTC dataset demonstrate the success of the method in detecting ICV regions and reducing FPs in CAD.

Index Terms— Colon CAD, Principle curvature flow, Bayesian methods, Ileocecal valve (ICV) detection

1. INTRODUCTION

The ileocecal valve (ICV) is located at the junction between the large and small bowel. The valve consists of two segments, an upper lip and a lower lip, that are formed by an intrusion of the circular muscle layer of the ileum into the lumen of the large intestine [1]. There are three types of ICVs differentiated by their shape and fat content. A labial ICV has a slit-like appearance and lower fat content, a papillary ICV has a dome-shaped appearance and also lower fat content, while a lipomatous ICV has variable shape but significant fatty tissue within the lips. A normal ICV of any type is defined as prominent when it protrudes far into the lumen of the large bowel, with the lips of the valve generally symmetric with respect to the valve orifice shown in Fig.1.

The ICV is a relatively small, deformable structure. In CT colonography (CTC) computer-aided detection of polyps, the ICV is a common source of false positives (FP), which may be time-consuming to interpret and exclude clinically. As reported in the most recent study for our colon CAD algorithm by Lawrence et al. [2], 18.8% of FP regions result from ICVs. Fig. 2 shows an example of an ICV being mistaken for a colon lesion in our colon CAD system [3]. Automatic detection of the ICV is therefore of great clinical value for improving the CAD performance. Moreover, identification of ICV provides an important clinical landmark to visualize the colon anatomy. However, detection of the ICV is challenging due to the ICV's bumpy polyp-like geometry and large shape and appearance variation.
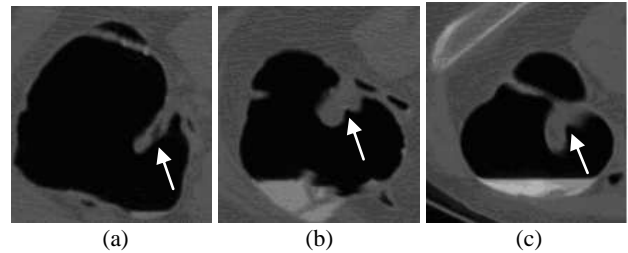
Fig.1. Examples of three different types of ICVs in CT images. (a) labial; (b) papillary; (c) lipomatous.

In the literature, there is limited work on ICV detection. Summers et al. [4] developed a CTC CAD approach for differentiating the ICV from a true polyp; however, the method is not fully automatic. Lu et al. [5] applied an incremental parameter learning (IPL) algorithm to detect the ICV in CTC images. Probabilistic boosting tree (PBT) and a large set (thousands) of point-level and box-level steerable features are used in a sequential search over location, pose and scale.

This paper proposes a novel and efficient concavity-based approach for the FP reduction of ICVs in CTC CAD. Different with the work in [5], we explicitly take advantage of the concavity of the ICV orifice, computing the concave region using a PDE flow and producing a very compact (six) set of features that are specific to the problem of ICV detection. The extracted orifice features, combined with Bayesian statistical features, are used in an Adaboost classifier to classify regions as ICV or non-ICV. Regions identified as ICV are removed from the set of findings produced by the CAD system. Our method has been evaluated on multi-center tagged CTC dataset and the experimental results demonstrate the method's success at FP reduction.
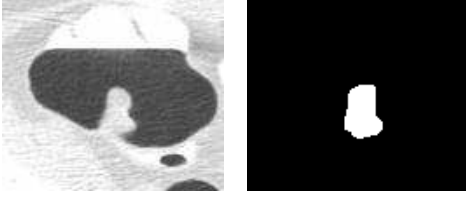
Fig.2. Example of a FP region in colon CAD. (left) CT sub-image; (right) FP region (the ICV is mistakenly detected as a polyp).

2. METHODOLOGY

In this section, we first apply a 3D second principal curvature based PDE for computing features based on the ICV orifice. In addition, we map the intensity and spatial location into a Bayesian framework to extract statistical features, and feed all features into a classifier to label regions as ICV or non-ICV.

2.1. Orifice features based on negative second principal curvature flow

The ICV orifice has an informative surface profile and it is considered a useful landmark [1] for the ICV identification. Our approach to extract orifice features is comprised of two stages. A negative second principal curvature flow is applied to extract 3D concave regions, which are subsequently refined using local geometry features.

Fig. 4(a) shows a typical ICV orifice in CTC. Note that the orifice is a round concave object embedded in the protruding ICV surface, which means its first and second principal curvatures are negative. In contrast, colonic folds are elongated structures, convex only in one direction and correspondingly exhibit a positive first principal curvature and a close to zero second principal curvature. Colonic polyps are convex and have positive values for both principal curvatures. van Wijk et al. [6] applied a positive second principal curvature PDE for polyp detection. In this paper, to extract ICV orifice feature, we instead propose a negative second principle curvature flow designed to detect concave regions. Repeated application of the PDE to the image will gradually flatten the surface and fill in the local concavities. In particular, the PDE is defined as

$$\frac{\partial I}{\partial t} = \begin{cases} -k_2(x_i) \cdot |\nabla I| & k_2(x_i) < 0 \\ 0 & k_2(x_i) \geq 0 \end{cases} \quad (1)$$

where $k_2(x_i)$ is the second principal curvature at voxel x_i, and $|\nabla I|$ is the gradient magnitude of the 3D image.

Based on Equation 1, the image intensities exhibit small (if any) change for colonic folds/polyps, and large change for concavities (such as the ICV orifice). During each iteration, only at locations of concave objects where the second principal curvature is negative, the image intensity is increased by an amount proportional to the local second

principle curvature k_2. After the PDE reaches steady state, the difference image D between the deformed and the original 3D image indicates the concave region.

Fig. 4(b) shows result of the PDE described in Equation 1. We note that the ICV orifice is successfully detected. However, as shown in Fig. 4(b), there are also other detected concave regions, which can be filtered out in a post-processing step, described next.

As mentioned previously, for normal ICVs, the lips of the valve are generally symmetric with respect to the valve orifice. Fig. 3 shows a schematic diagram of an ICV. Assume N_{colon} is the normal to the local protruding colon surface, $N_{orifice}$ is the normal to the ICV orifice, and $\alpha_{orifice}$ is an angle between the two normals.

To remove obvious non-ICV concave regions, the following geometric features are calculated:
1) We extract the protruding colon wall surface S_p (shown in Fig.3, Fig.4e) by subtracting the protruding object, which is obtained from the critical points based method applied to the segmented colon [3].
2) We calculate the average protruding surface normal N_{colon} (see Figure 3).
3) For each concave region obtained from Eq. 1, we calculate the average concave surface normal $N_{orifice}$.
4) Next, we calculate the orifice angle ($\alpha_{orifice}$) between the two normals.
5) A 3D distance transform is calculated from S_p. A maximum distance $fDisMax_{orifice}$ is then determined for each concave region.
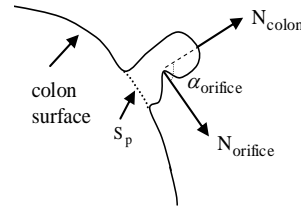

**Fig.3** A schematic diagram of an ICV orifice

In CTC, it is known that the ICV orifice is located on the side of the protruding object and between the two lips of the valve as shown in Fig. 1 and Fig. 4(a). Therefore, a concave region can be eliminated from the potential ICV orifice candidates if the maximum distance of the concave region is too close to the colon wall surface, namely, $fDisMax_{orifice} \leq \vartheta_{dis}$, or if the local concave surface direction is too close to the protruding surface normal, namely, $\alpha_{orifice} \leq \vartheta_{min}$, where ϑ_{dis} and ϑ_{min} are pre-defined thresholds. In this study, ϑ_{dis} is set to be 3mm, and ϑ_{min} is chosen to be $\pi/5$, which are determined experimentally.

For the remaining orifice candidates, three features including the number of concave regions, size, and orifice direction of the maximum concave region are calculated.

Fig. 4 shows an example of ICV orifice detection based on the above two steps. Fig. 5 is an example of a non-ICV concave region removed by the post-refinement step, due to the small concave angle α_{orifice}.
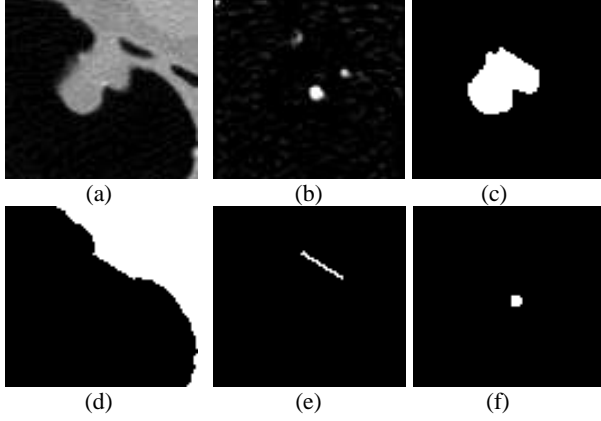
Fig. 4 Two-step ICV orifice detection example. (a) CT sub-image; (b) the difference image based on negative k2 PDE; (c) the protruding object extracted based on critical points [3]; (d) the local colon wall without the protruding object; (e) the protruding colon wall surface S_p; (f) the final detected ICV orifice after the post-refinement step.
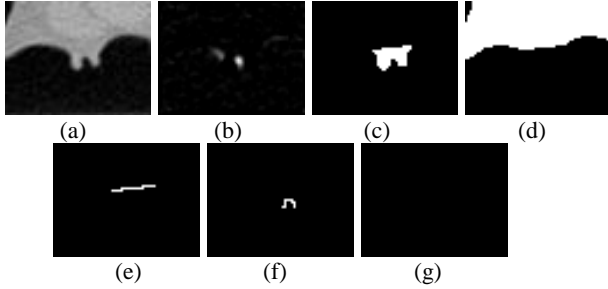
Fig. 5 Post-refinement step to remove a non-ICV concave region. (a-f) are the same as described in Fig.4; (g) is the final result indicating no ICV orifice detected.

2.2. Bayesian probability map for intensity and location features

Based on the clinical observation that most ICVs are positioned along the medial aspect of the cecum and have relatively low CT attenuation (often resulting from fat), image intensity and anatomic location provide additional features to discriminate ICVs from other protruding objects (e.g. colonic polyps). In this section, both intensity and location features are combined and then mapped into a probability calculation using a unified Bayesian framework.

A Gaussian function models the ICV intensity likelihood, defined as:

$$P\left(I|X\right) = \exp\left(-\frac{(I - \mu_{\text{I}})^2}{\delta_{\text{I}}^2}\right) \qquad (2)$$

where I is the image intensity at voxel X in 3D image, μ_{I} and δ_{I} are the mean and standard deviation (std), respectively. In our experiment, the mean μ_{I} is set to be $-20\,\text{HU}$, automatically determined using a training dataset.

ICVs are typically located near cecum (anatomically, the first part of the colon), far from the rectum (the last part). We employ this fact in a spatial location feature. First, a centerline through the colon is computed based on distance transforms [7]. For each potential region (protruding object), the distance to the rectum (L_{G}) is determined based on the centerline. A truncated Gaussian function models the ICV distance likelihood:

$$P\left(L_{\text{G}}|X\right) = \exp\left(-\frac{(L_{\text{G}} - \mu_{\text{DS}})^2}{\delta_{\text{DS}}^2}\right) \qquad (3)$$

where $L_{\text{G}} > \mu_{\text{DS}}$, $P\left(L_{\text{G}}|X\right) = 1$. Here, μ_{DS} and δ_{DS} are the mean and std, respectively, which are automatically determined from a training dataset.

Assuming both intensity and location features being conditionally independent, based on Bayes' law, the combined ICV probability map can be calculated as:

$$P\left(X|I, L_{\text{G}}|\right) = \frac{P\left(I|X\right) \cdot P\left(L_{\text{G}}|X\right) \cdot P\left(X\right)}{P\left(I\right) \cdot P\left(L_{\text{G}}\right)} \qquad (4)$$

where $P\left(X\right)$ is a prior probability. In this paper, a uniform prior is used.

2.3. ICV Classification using Adaboost

Given the regions from the CAD system and the corresponding feature vectors $\left\{F_i\right\}_{i=1,2,\ldots,N}$ calculated from the second principal curvature flow (Section 2.1) and the Bayesian probability map (Section 2.2), an AdaBoost classifier [8], which is a serial ensemble approach that forms a strong classifier with a linear combination of weak learners, is employed to distinguish ICV regions from the non-ICV regions. The ICV regions are then removed from the list of CAD findings. In this paper, six features (N=6) are computed, among which, three features are extracted from the PDE, namely, the orifice direction α_{orifice}, orifice size, and the number of the concave regions; and three statistical features from Bayesian probability map (mean, maximum and std of the probability within the region).

3. EXPERIMENTAL RESULTS

The proposed method has been trained and evaluated on multi-center tagged CTC images. In our previous work, we have developed a complete and automatic colon CAD system [3]. The aim of this experiment is to use the proposed method to remove ICV-type false regions.

The entire dataset is divided into a training set and an independent testing set. In the training set, there are 38 annotated CTC volumes from three different hospitals. Each ICV boundary was manually delineated by a qualified radiologist. The colon CAD system produces 316 potential lesion regions in total, among which, 29 regions correspond to the ICV. For each candidate region from CAD, the six features mentioned in Section 2 are calculated and fed into the Adaboost classifier. Table 1 shows the ICV detection performance on the training dataset. Note that 26 out of 29 ICVs are successfully detected based on the proposed method, resulting in an ICV detection sensitivity of 90%, with 25 FP regions.

In the independent testing dataset, there are 36 multi-center CTC volumes. To produce the ground truth, each polyp and ICV boundaries were manually delineated by qualified radiologists. In total, there are 202 potential lesion regions automatically detected by the CAD system, with 47 true positives and 155 false positive regions, resulting in FP ratio at 4.3/vol. Among those 155 FP regions, 30 regions correspond to the ICV, which means 19.4% FP regions are ICV regions.

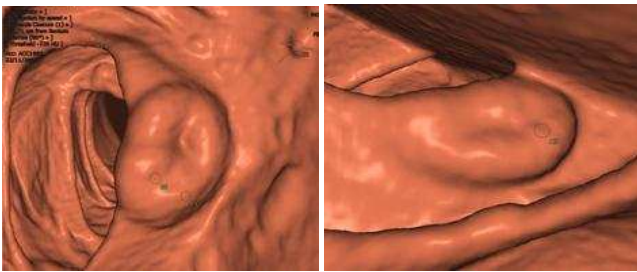**Table 1**. ICV detection performance of the proposed method on the training dataset

Number of ICV	Detected ICV	FP regions
29	26 (90%)	25

Table 2. The ICV detection performance of the proposed method on the independent testing dataset

Number of ICV	Detected ICV	FP regions
30	25 (83%)	24

Table 3. The comparative colon CAD performance before and after the proposed method on the testing dataset

Previous colon CAD		Colon CAD followed by the proposed method		
Number of polyps detected	FP (/vol)	Number of polyps detected	FP (/vol)	FP reduction
47	4.3	46	2.97	31%

Fig. 6 Example of the two detected ICVs in 3D.

The above trained model has been applied to the independent set. Table 2 shows ICV detection performance on the testing dataset. 25 of the 30 ICVs are successfully detected based on the proposed method, resulting in an ICV detection sensitivity of 83%. Of 24 non-ICV regions resulting from the classifier, only 1 of the 47 polyps is missing. This is a very encouraging result, as the CAD FP rate is thusly reduced from 4.3/vol down to 2.97/vol, which is about 31% FP reduction, as shown in Table 3. Thus, the proposed method is highly effective at removing FPs produced by the colon CAD system. Fig. 6 presents examples of detected ICVs

4. CONCLUSION

We have presented an automated, orifice-based detection method to identify ICV regions for FP reduction in CTC CAD. A second principal curvature based PDE is calculated to extract the ICV orifice feature. Then intensity and spatial features are combined and mapped into a probability calculation using a Bayesian framework.

The method has been applied to a multi-center tagged CTC dataset and shows the ICV detection rate of 90% for the training dataset and 83% for the independent testing data, with the FP reduction of 31% by using the proposed method. Tagged CT data are generally much more challenging. Both qualitative and quantitative experiment results demonstrate the clinical promise of the proposed method for removing a common source of false positive detections and improving colon CAD system performance.

5. REFERENCES

[1] D.Regge, T.M.Gallo, G.Nieddu, G.Galatola, M.Fracchia, E.Neri, P.Vagli, and C.Bartolozzi, "IIeocecal valve imaging on computed tomographic colonography", Abdominal Imaging, 30:20-25, 2004.

[2] E.M.Lawrence, P.J.Pickhardt, D.H.Kim and J.B.Robbins, "Colorectal polyps: stand-alone performance of computer-aided detection in a large asymptomatic screening population", Radiology, 256 (3): 791-798, Sep, 2010.

[3] G.Slabaugh, X.Yang, X.Ye, R.Boyes, and G.Beddoe, "A Robust and Fast System for CTC Computer-Aided Detection of Colorectal Lesions", Algorithms, 3(1): 21-43, 2010.

[4] R.M.Summers, J.Yao and C.D.Johnson, "CT Colonography with computer-aided detection: automated recognition of ileocecal valve to reduce number of false-positive detections", Radiology, 10, 2004.

[5] L.Lu, A.Barbu, M.Wolf, J.Liang, L.Bogoni, M.Salganicoff and D.Comaniciu, "Simultaneous detection and registration for ileocecal valve detection in 3D CT colonography", ECCV, 2006.

[6] C.van Wijk, V.F.van Ravesteijn, F.M.Vos and L.J.van Vliet," Detection and segmentation of colonic polyps on implicit isosurfaces by second principal curvature flow", IEEE Trans. Medical Imaging, 29 (3). 688-698, 2010.

[7] Y.Zhou and A.W.Toga, "Efficient skeletonization of volumetric objects", IEEE Trans. Visualization and computer graphics, 5(3), 196-209, 1999.

[8] Y.Freund, R.E.Scharpire. "A decision-theoretic generalization of on-line learning and an applization to boosting", Journal of computer and system sciences, 55, 119-139, 1997.